First Observation of Top Quark Production in the Forward Region

R. Aaij *et al.*[*]

(LHCb Collaboration)

Top quark production in the forward region in proton-proton collisions is observed for the first time. The $W + b$ final state with $W \rightarrow \mu\nu$ is reconstructed using muons with a transverse momentum, p_T, larger than 25 GeV in the pseudorapidity range $2.0 < \eta < 4.5$. The b jets are required to have $50 < p_T < 100$ GeV and $2.2 < \eta < 4.2$, while the transverse component of the sum of the muon and b-jet momenta must satisfy $p_T > 20$ GeV. The results are based on data corresponding to integrated luminosities of 1.0 and 2.0 fb^{-1} collected at center-of-mass energies of 7 and 8 TeV by LHCb. The inclusive top quark production cross sections in the fiducial region are $\sigma(\text{top})[7 \text{ TeV}] = 239 \pm 53(\text{stat}) \pm 33(\text{syst}) \pm 24(\text{theory})$ fb, $\sigma(\text{top})[8 \text{ TeV}] = 289 \pm 43(\text{stat}) \pm 40(\text{syst}) \pm 29(\text{theory})$ fb. These results, along with the observed differential yields and charge asymmetries, are in agreement with next-to-leading order standard model predictions.

The production of top quarks (t) from proton-proton (pp) collisions in the forward region is of considerable experimental and theoretical interest. In the standard model (SM), four processes make significant contributions to top quark production: $t\bar{t}$ pair production, single-top production via processes mediated by a W boson in the t channel ($qb \rightarrow q't$) or in the s channel ($q\bar{q}' \rightarrow t\bar{b}$), and single top produced in association with a W boson ($gb \rightarrow tW$). The initial-state b quarks arise from gluon splitting to $b\bar{b}$ pairs or from the intrinsic b quark content in the proton. Top quarks decay almost entirely via $t \rightarrow Wb$. The SM predicts that about 75% of $t \rightarrow Wb$ decays in the forward region are due to $t\bar{t}$ pair production. The remaining 25% are mostly due to t-channel single-top production, with s-channel and associated single-top production making percent-level contributions.

The enhancement at forward rapidities of $t\bar{t}$ production via $q\bar{q}$ and qg scattering, relative to gg fusion, can result in larger charge asymmetries, which may be sensitive to physics beyond the SM [1,2]. Forward $t\bar{t}$ events can be used to constrain the gluon parton distribution function (PDF) at a large momentum fraction, resulting in reduced theoretical uncertainty for many SM predictions [3]. Furthermore, both single-top and $t\bar{t}$ cross-section measurements in the forward region will provide important experimental tests of differential next-to-next-to-leading order theoretical calculations as they become available [4].

This Letter reports the first observation of top quark production in the forward region. The data used correspond to integrated luminosities of 1.0 and 2.0 fb^{-1} collected at center-of-mass energies of $\sqrt{s} = 7$ and 8 TeV in pp collisions with the LHCb detector. The W bosons are reconstructed using the $W \rightarrow \mu\nu$ decay with muons having a transverse momentum, p_T, larger than 25 GeV ($c = 1$ throughout this Letter) in the pseudorapidity range, $2.0 < \eta < 4.5$. The analysis is performed using jets clustered with the anti-k_T algorithm [5] using a distance parameter $R = 0.5$. The jets are required to have $50 < p_T < 100$ GeV and $2.2 < \eta < 4.2$. The muon and jet (j) must be separated by $\Delta R(\mu, j) > 0.5$, with $\Delta R \equiv \sqrt{\Delta\eta^2 + \Delta\phi^2}$. Here $\Delta\eta (\Delta\phi)$ is the difference in pseudorapidity (azimuthal angle) between the muon and jet momenta. The transverse component of the sum of the muon and jet momenta must satisfy $p_T(\mu + j) \equiv [\vec{p}(\mu) + \vec{p}(j)]_T > 20$ GeV.

The LHCb detector is a single-arm forward spectrometer covering the pseudorapidity range $2 < \eta < 5$, designed for the study of particles containing b or c quarks. It is described in detail in Refs. [6,7]. The trigger [8] consists of a hardware stage, based on information from the calorimeter and muon systems, followed by a software stage, which applies a full event reconstruction. This analysis requires at least one muon candidate that satisfies the trigger requirement of $p_T > 10$ GeV. Global event cuts (GECs), which prevent high-occupancy events from dominating the processing time of the software trigger, have an efficiency of about 90% for $W + $ jet and top quark events.

Simulated pp collisions are generated using PYTHIA [9] with an LHCb configuration [10]. Decays of hadronic particles are described by EVTGEN [11] in which final-state radiation is generated using PHOTOS [12]. The interaction of the generated particles with the detector, and its response, are implemented using the GEANT4 toolkit [13] as described in Ref. [14]. Further theory calculations are performed at
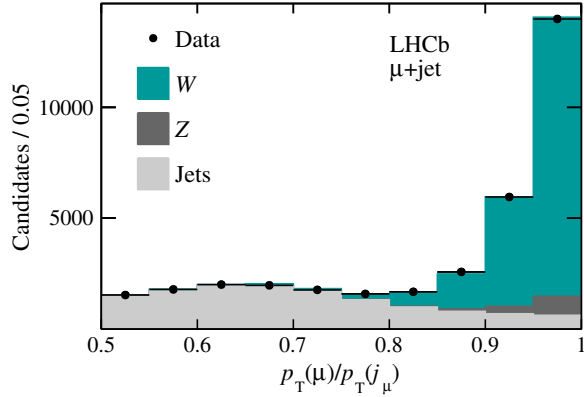
FIG. 1 (color online). Distribution of $p_T(\mu)/p_T(j_\mu)$ with fit overlaid for all $W + \text{jet}$ candidates.

next-to-leading order (NLO) with the MCFM package [15] and the CT10 PDF set [16], and are cross-checked using POWHEGBOX [17] with hadronization simulated by PYTHIA. The theoretical uncertainty on the cross-section predictions is a combination of PDF, scale, and strong-coupling (α_s) uncertainties. The PDF and scale uncertainties are evaluated following Refs. [16] and [18], respectively. The α_s uncertainty is evaluated as the envelope obtained using $\alpha_s(M_Z) \in [0.117, 0.118, 0.119]$ in the theory calculations.

The event selection is the same as that in Ref. [19] but a reduced fiducial region is used to enhance the top quark contribution relative to direct $W + b$ production. The signature for $W + \text{jet}$ events is an isolated high-p_T muon and a well-separated jet originating from the same pp interaction. Signal events are selected by requiring a high-p_T muon candidate and at least one jet with $\Delta R(\mu, j) > 0.5$. For each event, the highest-p_T muon candidate that satisfies the trigger requirements is selected, along with the highest-p_T jet from the same pp collision. The primary background to top quark production is direct $W + b$ production; however, $Z + b$ events, with one muon undetected in the decay $Z \to \mu\mu$, and di-b-jet events also contribute to the $\mu + b$-jet final state.

The anti-k_T clustering algorithm is used as implemented in FASTJET [20]. Information from all the detector subsystems is used to create charged and neutral particle inputs to the jet-clustering algorithm using a particle flow approach [21]. The reconstructed jets must fall within the pseudorapidity range $2.2 < \eta(j) < 4.2$. The reduced $\eta(j)$ acceptance ensures nearly uniform jet-reconstruction and heavy-flavor tagging efficiencies. The momentum of a reconstructed jet is corrected to obtain an unbiased estimate of the true jet momentum. The correction factor, typically between 0.9 and 1.1, is determined from simulation and depends on the jet p_T and η, the fraction of the jet p_T measured with the tracking system, and the number of pp interactions in the event.

The high-p_T muon candidate is not removed from the anti-k_T inputs and so is clustered into a jet. This jet, referred to as the muon jet and denoted as j_μ, is used to discriminate between $W + \text{jet}$ and dijet events [19]. No correction is applied to the momentum of the muon jet. The requirement $p_T(j_\mu + j) > 20$ GeV is made to suppress dijet backgrounds, which are well balanced in p_T, unlike $W + \text{jet}$ events, where there is undetected energy from the neutrino. Events with a second, oppositely charged, high-p_T muon candidate from the same pp collision are vetoed. However, when the dimuon invariant mass is in the range $60 < M(\mu^+\mu^-) < 120$ GeV, such events are selected as $Z(\mu\mu) + \text{jet}$ candidates, which are used to determine the $Z + \text{jet}$ background.

The jets are identified (tagged) as originating from the hadronization of a b or c quark by the presence of a secondary vertex (SV) with $\Delta R < 0.5$ between the jet axis and the SV direction of flight, defined by the vector from the pp interaction point to the SV position. Two boosted decision trees (BDTs) [22,23], trained on the characteristics of the SV and the jet, are used to separate heavy-flavor jets from light-parton jets, and to separate b jets from c jets. The two-dimensional distribution of the BDT responses observed in data is fitted to obtain the SV-tagged b, c, and light-parton jet yields. The SV-tagger algorithm is described in Ref. [24], where the heavy-flavor tagging efficiencies and light-parton mistag probabilities are measured in data. The data samples used in Ref. [24] are too small to validate the performance of the SV-tagger algorithm in the $p_T(j) > 100$ GeV region. Furthermore, the mistag probability of light-parton jets increases with jet p_T. Therefore, only jets with $p_T < 100$ GeV are considered in the fiducial region, which, according to simulation, retains about 80% of all top quark events.

Inclusive $W + \text{jet}$ production, i.e., where no SV-tag requirement is made on the jet, is only contaminated at the percent level by processes other than direct $W + \text{jet}$ production. Therefore, $W + \text{jet}$ production is used to validate both the theory predictions and the modeling of the detector response. Furthermore, the SM prediction for $\sigma(Wb)/\sigma(Wj)$ has a smaller relative uncertainty than $\sigma(Wb)$ alone, since the theory uncertainties partially cancel in the ratio. The analysis strategy is to first measure the $W + \text{jet}$ yields, and then to obtain predictions for the yields of direct $W + b$ production using the prediction for $\sigma(Wb)/\sigma(Wj)$. To an excellent approximation, many experimental effects, e.g., the muon reconstruction efficiency, are expected to be the same for both samples and do not need to be considered in the direct $W + b$ yield prediction.

The $W + \text{jet}$ yield is determined by performing a fit to the $p_T(\mu)/p_T(j_\mu)$ distribution with templates, histograms obtained from data, as described in Ref. [19]. The $Z + \text{jet}$ contribution is fixed from the fully reconstructed $Z(\mu\mu) + \text{jet}$ yield, where the probability for one of the muons to escape detection is obtained using simulation. The contributions of b, c, and light-parton jets are each free to vary
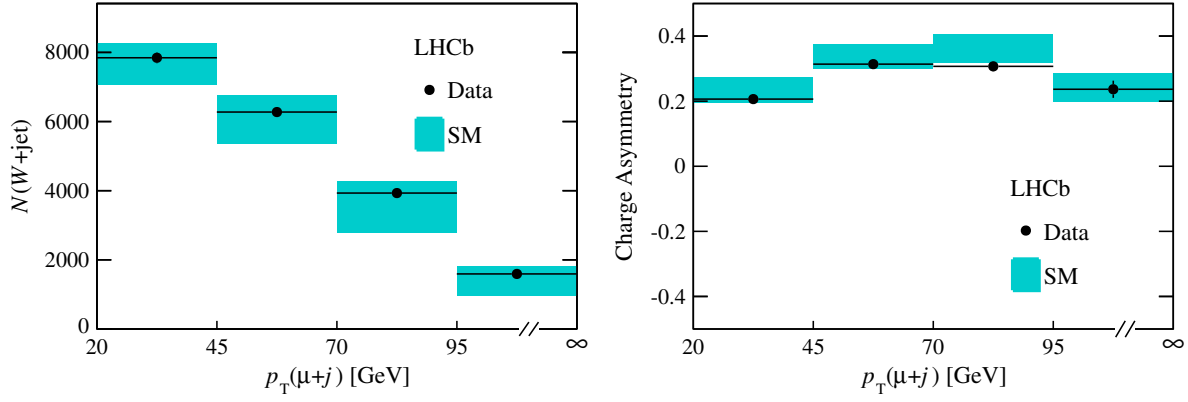
FIG. 2 (color online).   Results for the inclusive $W + \text{jet}$ yield (left) and charge asymmetry (right) versus $p_T(\mu + j)$ compared to SM predictions at NLO obtained using MCFM. The data error bars are smaller than the marker size; the SM uncertainties are highly correlated across $p_T(\mu + j)$ bins.

in the fit. Figure 1 shows the fit for all candidates in the data sample. Such a fit is performed for each muon charge separately in bins of $p_T(\mu + j)$; the differential $W + \text{jet}$ yield and charge asymmetry, defined as $[\sigma(W^+ j) - \sigma(W^- j)]/[\sigma(W^+ j) + \sigma(W^- j)]$, are given in Fig. 2.

To compare the data to theory predictions, the detector response must be taken into account. All significant aspects of the detector response are determined using data-driven techniques. The muon trigger, reconstruction, and selection efficiencies are determined using $Z \to \mu\mu$ events [21,25]. The GEC efficiency is obtained following Ref. [21]: an alternative dimuon trigger requirement, which requires a looser GEC, is used to determine the fraction of events that are rejected. Contamination from $W \to \tau \to \mu$ decays are estimated to be 2.5% using both simulated $W + \text{jet}$ events and inclusive W data samples [26]. The fraction of muons that migrate out of the fiducial region due to final-state radiation is about 1.5% [26].

Migration of events in jet p_T due to the detector response is studied with a data sample enriched in b jets using SV tagging. The $p_T(\text{SV})/p_T(j)$ distribution observed in data is compared to templates obtained from simulation in bins of jet p_T. The resolution and scale for each jet p_T bin are varied in simulation to find the best description of the data and to construct a detector response matrix. Figure 2 shows that the SM predictions, obtained with all detector response effects applied, agree with the inclusive $W + \text{jet}$ data.

The yields of $W + c$ and $W + b$, which includes $t \to Wb$ decays, are determined using the subset of candidates with a SV-tagged jet and binned according to $p_T(\mu)/p_T(j_\mu)$. In each $p_T(\mu)/p_T(j_\mu)$ bin, the two-dimensional SV-tagger BDT-response distributions are fitted to determine the yields of c-tagged and b-tagged jets, which are used to form the $p_T(\mu)/p_T(j_\mu)$ distributions for candidates with c-tagged and b-tagged jets. These $p_T(\mu)/p_T(j_\mu)$ distributions are fitted to determine the SV-tagged $W + c$ and $W + b$ yields.

A fit to the $p_T(\mu)/p_T(j_\mu)$ distribution built from the c-tagged jets from the full data sample is provided as Supplemental Material to this Letter [27]. Figure 3 shows that the $W + c$ yield versus $p_T(\mu + c)$ agrees with the SM prediction. Since the $W + c$ final state does not have any significant contributions from diboson or top quark production in the SM, this comparison validates the analysis procedures.

Figure 4 shows a fit to the $p_T(\mu)/p_T(j_\mu)$ distribution built from the b-tagged jets from the full data sample. For $p_T(\mu)/p_T(j_\mu) > 0.9$ the data are dominantly from W decays. Figure 5 shows the yield and charge asymmetry distributions obtained as a function of $p_T(\mu + b)$. The direct $W + b$ prediction is determined by scaling the inclusive $W + \text{jet}$ distribution observed in data by the SM prediction for $\sigma(Wb)/\sigma(Wj)$ and by the b-tagging efficiency measured in data [24]. As can be seen, the data cannot be described by the expected direct $W + b$ contribution alone. The observed yield is about 3 times larger than the SM prediction without a top quark contribution,
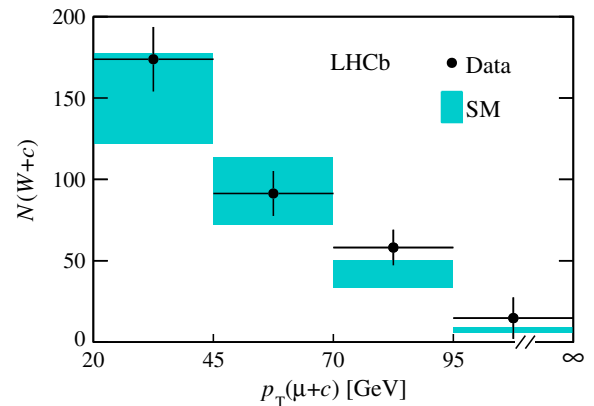

FIG. 3 (color online).   Results for $W + c$ compared to SM predictions at NLO obtained using MCFM.
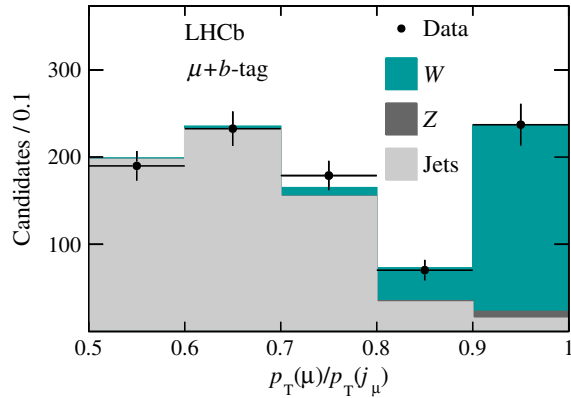
FIG. 4 (color online). Distribution of $p_T(\mu)/p_T(j_\mu)$ with fit overlaid for all $W + b$ candidates.

while the SM prediction including both $t\bar{t}$ and single-top production does describe the data well.

In Ref. [19], $W + b$ is studied in a larger fiducial region $[p_T(\mu) > 20$ GeV, $p_T(j) > 20$ GeV$]$, where the top quark contribution is expected to be about half as large as that of direct $W+b$ production. The ratio $[\sigma(Wb)+\sigma(\text{top})]/\sigma(Wj)$ is measured in the larger fiducial region to be 1.17 ± 0.13 (stat) ± 0.18 (syst)% at $\sqrt{s} = 7$ TeV and 1.29 ± 0.08 (stat) ± 0.19 (syst)% at $\sqrt{s} = 8$ TeV. These results agree with SM predictions, which include top quark production, of $1.23 \pm 0.24\%$ and $1.38 \pm 0.26\%$, respectively. This validates the direct $W + b$ prediction, since direct $W + b$ production is the dominant contribution to the larger fiducial region.

Various sources of systematic uncertainties are considered and summarized in Table I. The direct $W + b$ prediction is normalized using the observed inclusive $W + $ jet data yields. Therefore, most experimental systematic uncertainties cancel to a good approximation.

Since the muon kinematic distributions in $W + $ jet and $W + b$ are similar, all muon-based uncertainties are negligible with the exception of the trigger GEC efficiency.

The data-driven GEC study discussed above shows that the efficiencies are consistent for $W + $ jet and $W + b$, with the statistical precision of this study assigned as the systematic uncertainty. Mismodeling of the $p_T(\mu)/p_T(j_\mu)$ distributions largely cancels, since this shifts the inclusive $W + $ jet and $W + b$ final-state yields by the same amount, leaving the observed excess over the expected direct $W + b$ yield unaffected. The one exception is possible mismodeling of the dijet templates, since the flavor content of the dijet background is not the same in the two samples. Variations of these templates are considered and a relative uncertainty of 5% is assigned on the W boson yields.

The jet-reconstruction efficiencies for heavy-flavor and light-parton jets in simulation are found to be consistent within 2%, which is assigned as the systematic uncertainty for flavor dependencies in the jet-reconstruction efficiency. The SV-tagger BDT templates used in this analysis are two-dimensional histograms obtained from the data samples enriched in b and c jets used in Ref. [24]. Following Refs. [19,24], a 5% uncertainty on the b-tagged yields is assigned due to uncertainty in these templates. The precision of the b-tagging efficiency measurement (10%) in data [24] is assigned as an additional uncertainty.

To determine the statistical significance of the top quark contribution, a binned profile likelihood test is performed. The top quark distribution and charge asymmetry versus $p_T(\mu + b)$ are obtained from the SM predictions. The total top quark yield is allowed to vary freely. Systematic uncertainties, both theoretical and experimental, are handled as Gaussian constraints. The profile likelihood technique is used to compare the SM hypotheses with and without a top quark contribution. The significance obtained using Wilks theorem [28] is 5.4σ, confirming the observation of top quark production in the forward region.

The yield and charge asymmetry distributions versus $p_T(\mu + b)$ observed at $\sqrt{s} = 7$ and 8 TeV are each consistent with the SM predictions. The excess of the observed yield relative to the direct $W + b$ prediction at each $\sqrt{s}$ is attributed to top quark production, and used to
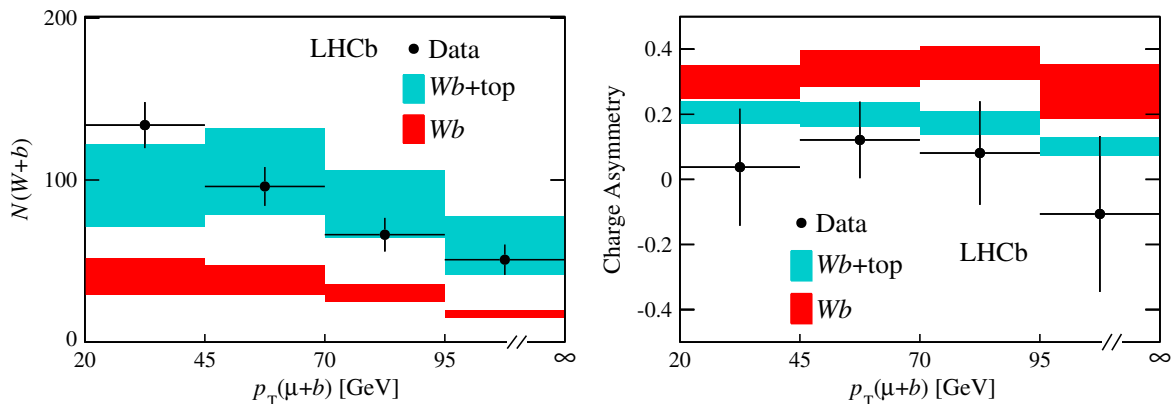

FIG. 5 (color online). Results for the $W + b$ yield (left) and charge asymmetry (right) versus $p_T(\mu + b)$ compared to SM predictions obtained at NLO using MCFM.

TABLE I.   Relative systematic uncertainties.

Source	Uncertainty
GEC	2%
$p_T(\mu)/p_T(j_\mu)$ templates	5%
Jet reconstruction	2%
SV-tag BDT templates	5%
b-tag efficiency	10%
Trigger and μ selection	2%[a]
Jet energy	5%[a]
$W \to \tau \to \mu$	1%[a]
Luminosity	1%–2%[a]
Total	14%
Theory	10%

[a]An uncertainty that only applies to the cross-section measurement
and not the significance determination. Only the luminosity
uncertainty depends on $\sqrt{s}$: 2% at 7 TeV and 1% at 8 TeV.

measure the cross sections. Some additional systematic
uncertainties that apply to the cross-section measurements
do not factor into the significance determination. The
uncertainties due to the muon trigger, reconstruction, and
selection efficiencies are taken from the data-driven studies
of Refs. [21,25]. The uncertainty due to the jet energy
determination is obtained from the data-driven study used
to obtain the detector response matrix. The uncertainty due
to $W \to \tau \to \mu$ contamination is taken as the difference
between the contamination in simulation versus that of a
data-driven study of inclusive $W \to \mu\nu$ production [26].
The luminosity uncertainty is described in detail in
Ref. [29]. The total systematic uncertainty is obtained by
adding the individual contributions in quadrature.

The resulting inclusive top production cross sections in
the fiducial region defined by $p_T(\mu) > 25$ GeV,
$2.0 < \eta(\mu) < 4.5$, $50 < p_T(b) < 100$ GeV, $2.2 < \eta(b) < 4.2$, $\Delta R(\mu, b) > 0.5$, and $p_T(\mu + b) > 20$ GeV, are

$$\sigma(\text{top})[7\text{ TeV}] = 239 \pm 53\,(\text{stat}) \pm 33\,(\text{syst}) \pm 24\,(\text{theory})\text{ fb},$$

$$\sigma(\text{top})[8\text{ TeV}] = 289 \pm 43\,(\text{stat}) \pm 40\,(\text{syst}) \pm 29\,(\text{theory})\text{ fb}.$$

The systematic uncertainties are nearly 100% correlated
between the two measurements.

In summary, top quark production is observed for the
first time in the forward region. The cross-section results
are in agreement with the SM predictions of
$180^{+51}_{-41}(312^{+83}_{-68})$ fb at 7(8) TeV obtained at NLO using
MCFM. The differential distributions of the yield and
charge asymmetry are also consistent with SM predictions.

[1] A. L. Kagan, J. F. Kamenik, G. Perez, and S. Stone, Probing
New Top Physics at the LHCb Experiment, Phys. Rev. Lett.
107, 082003 (2011).

[2] R. Gauld, Leptonic Top quark asymmetry predictions at
LHCb, Phys. Rev. D **91**, 054029 (2015).

[3] R. Gauld, Feasibility of top quark measurements at LHCb
and constraints on the large-x gluon PDF, J. High Energy
Phys. 02 (2014) 126.

[4] M. Czakon, P. Fiedler, and A. Mitov, Resolving the Tevatron
Top Quark Forward-Backward Asymmetry Puzzle: Fully
Differential Next-to-Next-to-Leading-Order Calculation,
Phys. Rev. Lett. **115**, 052001 (2015).

[5] M. Cacciari, G. P. Salam, and G. Soyez, The anti-k_t jet
clustering algorithm, J. High Energy Phys. 04 (2008)
063.

[6] A. A. Alves Jr. *et al.* (LHCb Collaboration), The LHCb
detector at the LHC, JINST **3**, S08005 (2008).

[7] R. Aaij *et al.* (LHCb Collaboration), LHCb detector
performance, Int. J. Mod. Phys. A **30**, 1530022 (2015).

[8] R. Aaij *et al.*, The LHCb trigger and its performance in
2011, JINST **8**, P04022 (2013).

[9] T. Sjöstrand, S. Mrenna, and P. Skands, PYTHIA 6.4
physics and manual, J. High Energy Phys. 05 (2006)
026; , A brief introduction to PYTHIA 8.1, Comput. Phys.
Commun. **178**, 852 (2008).

[10] I. Belyaev *et al.*, Handling of the generation of primary
events in Gauss, the LHCb simulation framework, J. Phys.
Conf. Ser. **331**, 032047 (2011).

[11] D. J. Lange, The EvtGen particle decay simulation package,
Nucl. Instrum. Methods Phys. Res., Sect. A **462**, 152
(2001).

[12] P. Golonka and Z. Was, PHOTOS Monte Carlo: A precision
tool for QED corrections in Z and W decays, Eur. Phys. J. C
45, 97 (2006).

[13] J. Allison *et al.* (Geant4 Collaboration), Geant4 developments and applications, IEEE Trans. Nucl. Sci. **53**, 270 (2006); S. Agostinelli *et al.* (Geant4 Collaboration), Geant4: A simulation toolkit, Nucl. Instrum. Methods Phys. Res., Sect. A **506**, 250 (2003).

[14] M. Clemencic, G. Corti, S. Easo, C. R. Jones, S. Miglioranzi, M. Pappagallo, and P. Robbe, The LHCb simulation application, Gauss: Design, evolution and experience, J. Phys. Conf. Ser. **331**, 032023 (2011).

[15] J. M. Campbell and R. K. Ellis, Radiative corrections to $Zb\bar{b}$ production, Phys. Rev. D **62**, 114012 (2000).

[16] H.-L. Lai, M. Guzzi, J. Huston, Z. Li, P. M. Nadolsky, J. Pumplin, and C.-P. Yuan, New parton distributions for collider physics, Phys. Rev. D **82**, 074024 (2010).

[17] S. Alioli, P. Nason, C. Oleari, and E. Re, A general framework for implementing NLO calculations in shower Monte Carlo programs: The POWHEG BOX, J. High Energy Phys. 06 (2010) 043.

[18] K. Hamilton, P. Nason, E. Re, and G. Zanderighi, NNLOPS simulation of Higgs boson production, J. High Energy Phys. 10 (2013) 222.

[19] R. Aaij *et al.* (LHCb Collaboration), Study of W boson production in association with beauty and charm, Phys. Rev. D **92**, 052001 (2015).

[20] M. Cacciari, G. P. Salam, and G. Soyez, FastJet user manual, Eur. Phys. J. C **72**, 1896 (2012).

[21] R. Aaij *et al.* (LHCb Collaboration), Study of forward $Z + $ jet production in pp collisions at $\sqrt{s} = 7$ TeV, J. High Energy Phys. 01 (2014) 033.

[22] L. Breiman, J. H. Friedman, R. A. Olshen, and C. J. Stone, *Classification and Regression Trees* (Wadsworth International Group, Belmont, CA, 1984).

[23] R. E. Schapire and Y. Freund, A decision-theoretic generalization of on-line learning and an application to boosting, J. Comput. Syst. Sci. **55**, 119 (1997).

[24] R. Aaij *et al.* (LHCb Collaboration), Identification of beauty and charm quark jets at LHCb, JINST **10**, P06013 (2015).

[25] R. Aaij *et al.* (LHCb Collaboration), Measurement of the forward Z boson cross-section in pp collisions at $\sqrt{s} = 7$ TeV, J. High Energy Phys. 08 (2015) 039.

[26] R. Aaij *et al.* (LHCb Collaboration), Measurement of the forward W boson production cross-section in pp collisions at $\sqrt{s} = 7$ TeV, J. High Energy Phys. 12 (2014) 079.

[27] See Supplemental Material at http://link.aps.org/supplemental/10.1103/PhysRevLett.115.112001 for distribution of $p_T(\mu)/p_T(j_\mu)$ with fit overlaid for all $W + c$ candidates.

[28] S. S. Wilks, The large-sample distribution of the likelihood ratio for testing composite hypotheses, Ann. Math. Stat. **9**, 60 (1938).

[29] R. Aaij *et al.* (LHCb Collaboration), Precision luminosity measurements at LHCb, JINST **9**, P12005 (2014).

R. Aaij,[38] B. Adeva,[37] M. Adinolfi,[46] A. Affolder,[52] Z. Ajaltouni,[5] S. Akar,[6] J. Albrecht,[9] F. Alessio,[38] M. Alexander,[51] S. Ali,[41] G. Alkhazov,[30] P. Alvarez Cartelle,[53] A. A. Alves Jr.,[57] S. Amato,[2] S. Amerio,[22] Y. Amhis,[7] L. An,[3] L. Anderlini,[17,a] J. Anderson,[40] M. Andreotti,[16,b] J. E. Andrews,[58] R. B. Appleby,[54] O. Aquines Gutierrez,[10] F. Archilli,[38] P. d'Argent,[11] A. Artamonov,[35] M. Artuso,[59] E. Aslanides,[6] G. Auriemma,[25,c] M. Baalouch,[5] S. Bachmann,[11] J. J. Back,[48] A. Badalov,[36] C. Baesso,[60] W. Baldini,[16,38] R. J. Barlow,[54] C. Barschel,[38] S. Barsuk,[7] W. Barter,[38] V. Batozskaya,[28] V. Battista,[39] A. Bay,[39] L. Beaucourt,[4] J. Beddow,[51] F. Bedeschi,[23] I. Bediaga,[1] L. J. Bel,[41] I. Belyaev,[31] E. Ben-Haim,[8] G. Bencivenni,[18] S. Benson,[38] J. Benton,[46] A. Berezhnoy,[32] R. Bernet,[40] A. Bertolin,[22] M.-O. Bettler,[38] M. van Beuzekom,[41] A. Bien,[11] S. Bifani,[45] T. Bird,[54] A. Birnkraut,[9] A. Bizzeti,[17,d] T. Blake,[48] F. Blanc,[39] J. Blouw,[10] S. Blusk,[59] V. Bocci,[25] A. Bondar,[34] N. Bondar,[30,38] W. Bonivento,[15] S. Borghi,[54] M. Borsato,[7] T. J. V. Bowcock,[52] E. Bowen,[40] C. Bozzi,[16] S. Braun,[11] D. Brett,[54] M. Britsch,[10] T. Britton,[59] J. Brodzicka,[54] N. H. Brook,[46] A. Bursche,[40] J. Buytaert,[38] S. Cadeddu,[15] R. Calabrese,[16,b] M. Calvi,[20,e] M. Calvo Gomez,[36,f] P. Campana,[18] D. Campora Perez,[38] L. Capriotti,[54] A. Carbone,[14,g] G. Carboni,[24,h] R. Cardinale,[19,i] A. Cardini,[15] P. Carniti,[20] L. Carson,[50] K. Carvalho Akiba,[2,38] G. Casse,[52] L. Cassina,[20,e] L. Castillo Garcia,[38] M. Cattaneo,[38] Ch. Cauet,[9] G. Cavallero,[19] R. Cenci,[23,j] M. Charles,[8] Ph. Charpentier,[38] M. Chefdeville,[4] S. Chen,[54] S.-F. Cheung,[55] N. Chiapolini,[40] M. Chrzaszcz,[40] X. Cid Vidal,[38] G. Ciezarek,[41] P. E. L. Clarke,[50] M. Clemencic,[38] H. V. Cliff,[47] J. Closier,[38] V. Coco,[38] J. Cogan,[6] E. Cogneras,[5] V. Cogoni,[15,k] L. Cojocariu,[29] G. Collazuol,[22] P. Collins,[38] A. Comerma-Montells,[11] A. Contu,[15,38] A. Cook,[46] M. Coombes,[46] S. Coquereau,[8] G. Corti,[38] M. Corvo,[16,b] B. Couturier,[38] G. A. Cowan,[50] D. C. Craik,[48] A. Crocombe,[48] M. Cruz Torres,[60] S. Cunliffe,[53] R. Currie,[53] C. D'Ambrosio,[38] J. Dalseno,[46] P. N. Y. David,[41] A. Davis,[57] K. De Bruyn,[41] S. De Capua,[54] M. De Cian,[11] J. M. De Miranda,[1] L. De Paula,[2] W. De Silva,[57] P. De Simone,[18] C.-T. Dean,[51] D. Decamp,[4] M. Deckenhoff,[9] L. Del Buono,[8] N. Déléage,[4] M. Demmer,[9] D. Derkach,[55] O. Deschamps,[5] F. Dettori,[38] A. Di Canto,[38] F. Di Ruscio,[24] H. Dijkstra,[38] S. Donleavy,[52] F. Dordei,[11] M. Dorigo,[39] A. Dosil Suárez,[37] D. Dossett,[48] A. Dovbnya,[43] K. Dreimanis,[52] L. Dufour,[41] G. Dujany,[54] F. Dupertuis,[39] P. Durante,[38] R. Dzhelyadin,[35] A. Dziurda,[26] A. Dzyuba,[30] S. Easo,[49,38] U. Egede,[53] V. Egorychev,[31] S. Eidelman,[34] S. Eisenhardt,[50] U. Eitschberger,[9] R. Ekelhof,[9] L. Eklund,[51] I. El Rifai,[5] Ch. Elsasser,[40] S. Ely,[59] S. Esen,[11] H. M. Evans,[47] T. Evans,[55] A. Falabella,[14] C. Färber,[11] C. Farinelli,[41] N. Farley,[45]

S. Farry,[52] R. Fay,[52] D. Ferguson,[50] V. Fernandez Albor,[37] F. Ferrari,[14] F. Ferreira Rodrigues,[1] M. Ferro-Luzzi,[38] S. Filippov,[33] M. Fiore,[16,38,b] M. Fiorini,[16,b] M. Firlej,[27] C. Fitzpatrick,[39] T. Fiutowski,[27] K. Fohl,[38] P. Fol,[53] M. Fontana,[10] F. Fontanelli,[19,i] R. Forty,[38] O. Francisco,[2] M. Frank,[38] C. Frei,[38] M. Frosini,[17] J. Fu,[21] E. Furfaro,[24,h] A. Gallas Torreira,[37] D. Galli,[14,g] S. Gallorini,[22,38] S. Gambetta,[50] M. Gandelman,[2] P. Gandini,[55] Y. Gao,[3] J. García Pardiñas,[37] J. Garofoli,[59] J. Garra Tico,[47] L. Garrido,[36] D. Gascon,[36] C. Gaspar,[38] U. Gastaldi,[16] R. Gauld,[55] L. Gavardi,[9] G. Gazzoni,[5] A. Geraci,[21,l] D. Gerick,[11] E. Gersabeck,[11] M. Gersabeck,[54] T. Gershon,[48] Ph. Ghez,[4] A. Gianelle,[22] S. Gianì,[39] V. Gibson,[47] O. G. Girard,[39] L. Giubega,[29] V. V. Gligorov,[38] C. Göbel,[60] D. Golubkov,[31] A. Golutvin,[53,31,38] A. Gomes,[1,m] C. Gotti,[20,e] M. Grabalosa Gándara,[5] R. Graciani Diaz,[36] L. A. Granado Cardoso,[38] E. Graugés,[36] E. Graverini,[40] G. Graziani,[17] A. Grecu,[29] E. Greening,[55] S. Gregson,[47] P. Griffith,[45] L. Grillo,[11] O. Grünberg,[63] B. Gui,[59] E. Gushchin,[33] Yu. Guz,[35,38] T. Gys,[38] T. Hadavizadeh,[55] C. Hadjivasiliou,[59] G. Haefeli,[39] C. Haen,[38] S. C. Haines,[47] S. Hall,[53] B. Hamilton,[58] T. Hampson,[46] X. Han,[11] S. Hansmann-Menzemer,[11] N. Harnew,[55] S. T. Harnew,[46] J. Harrison,[54] J. He,[38] T. Head,[39] V. Heijne,[41] K. Hennessy,[52] P. Henrard,[5] L. Henry,[8] J. A. Hernando Morata,[37] E. van Herwijnen,[38] M. Heß,[63] A. Hicheur,[2] D. Hill,[55] M. Hoballah,[5] C. Hombach,[54] W. Hulsbergen,[41] T. Humair,[53] N. Hussain,[55] D. Hutchcroft,[52] D. Hynds,[51] M. Idzik,[27] P. Ilten,[56] R. Jacobsson,[38] A. Jaeger,[11] J. Jalocha,[55] E. Jans,[41] A. Jawahery,[58] F. Jing,[3] M. John,[55] D. Johnson,[38] C. R. Jones,[47] C. Joram,[38] B. Jost,[38] N. Jurik,[59] S. Kandybei,[43] W. Kanso,[6] M. Karacson,[38] T. M. Karbach,[38] S. Karodia,[51] M. Kelsey,[59] I. R. Kenyon,[45] M. Kenzie,[38] T. Ketel,[42] B. Khanji,[20,38,e] C. Khurewathanakul,[39] S. Klaver,[54] K. Klimaszewski,[28] O. Kochebina,[7] M. Kolpin,[11] I. Komarov,[39] R. F. Koopman,[42] P. Koppenburg,[41,38] M. Korolev,[32] M. Kozeiha,[5] L. Kravchuk,[33] K. Kreplin,[11] M. Kreps,[48] G. Krocker,[11] P. Krokovny,[34] F. Kruse,[9] W. Kucewicz,[26,n] M. Kucharczyk,[26] V. Kudryavtsev,[34] A. K. Kuonen,[39] K. Kurek,[28] T. Kvaratskheliya,[31] V. N. La Thi,[39] D. Lacarrere,[38] G. Lafferty,[54] A. Lai,[15] D. Lambert,[50] R. W. Lambert,[42] G. Lanfranchi,[18] C. Langenbruch,[48] B. Langhans,[38] T. Latham,[48] C. Lazzeroni,[45] R. Le Gac,[6] J. van Leerdam,[41] J.-P. Lees,[4] R. Lefèvre,[5] A. Leflat,[32,38] J. Lefrançois,[7] O. Leroy,[6] T. Lesiak,[26] B. Leverington,[11] Y. Li,[7] T. Likhomanenko,[65,64] M. Liles,[52] R. Lindner,[38] C. Linn,[38] F. Lionetto,[40] B. Liu,[15] X. Liu,[3] D. Loh,[48] S. Lohn,[38] I. Longstaff,[51] J. H. Lopes,[2] D. Lucchesi,[22,o] M. Lucio Martinez,[37] H. Luo,[50] A. Lupato,[22] E. Luppi,[16,b] O. Lupton,[55] F. Machefert,[7] F. Maciuc,[29] O. Maev,[30] K. Maguire,[54] S. Malde,[55] A. Malinin,[64] G. Manca,[7] G. Mancinelli,[6] P. Manning,[59] A. Mapelli,[38] J. Maratas,[5] J. F. Marchand,[4] U. Marconi,[14] C. Marin Benito,[36] P. Marino,[23,38,j] R. Märki,[39] J. Marks,[11] G. Martellotti,[25] M. Martin,[6] M. Martinelli,[39] D. Martinez Santos,[42] F. Martinez Vidal,[66] D. Martins Tostes,[2] A. Massafferri,[1] R. Matev,[38] A. Mathad,[48] Z. Mathe,[38] C. Matteuzzi,[20] K. Matthieu,[11] A. Mauri,[40] B. Maurin,[39] A. Mazurov,[45] M. McCann,[53] J. McCarthy,[45] A. McNab,[54] R. McNulty,[12] B. Meadows,[57] F. Meier,[9] M. Meissner,[11] D. Melnychuk,[28] M. Merk,[41] D. A. Milanes,[62] M.-N. Minard,[4] D. S. Mitzel,[11] J. Molina Rodriguez,[60] S. Monteil,[5] M. Morandin,[22] P. Morawski,[27] A. Mordà,[6] M. J. Morello,[23,j] J. Moron,[27] A. B. Morris,[50] R. Mountain,[59] F. Muheim,[50] J. Müller,[9] K. Müller,[40] V. Müller,[9] M. Mussini,[14] B. Muster,[39] P. Naik,[46] T. Nakada,[39] R. Nandakumar,[49] A. Nandi,[55] I. Nasteva,[2] M. Needham,[50] N. Neri,[21] S. Neubert,[11] N. Neufeld,[38] M. Neuner,[11] A. D. Nguyen,[39] T. D. Nguyen,[39] C. Nguyen-Mau,[39,p] V. Niess,[5] R. Niet,[9] N. Nikitin,[32] T. Nikodem,[11] D. Ninci,[23] A. Novoselov,[35] D. P. O'Hanlon,[48] A. Oblakowska-Mucha,[27] V. Obraztsov,[35] S. Ogilvy,[51] O. Okhrimenko,[44] R. Oldeman,[15,k] C. J. G. Onderwater,[67] B. Osorio Rodrigues,[1] J. M. Otalora Goicochea,[2] A. Otto,[38] P. Owen,[53] A. Oyanguren,[66] A. Palano,[13,q] F. Palombo,[21,r] M. Palutan,[18] J. Panman,[38] A. Papanestis,[49] M. Pappagallo,[51] L. L. Pappalardo,[16,b] C. Pappenheimer,[57] C. Parkes,[54] G. Passaleva,[17] G. D. Patel,[52] M. Patel,[53] C. Patrignani,[19,i] A. Pearce,[54,49] A. Pellegrino,[41] G. Penso,[25,s] M. Pepe Altarelli,[38] S. Perazzini,[14,g] P. Perret,[5] L. Pescatore,[45] K. Petridis,[46] A. Petrolini,[19,i] M. Petruzzo,[21] E. Picatoste Olloqui,[36] B. Pietrzyk,[4] T. Pilař,[48] D. Pinci,[25] A. Pistone,[19] A. Piucci,[11] S. Playfer,[50] M. Plo Casasus,[37] T. Poikela,[38] F. Polci,[8] A. Poluektov,[48,34] I. Polyakov,[31] E. Polycarpo,[2] A. Popov,[35] D. Popov,[10,38] B. Popovici,[29] C. Potterat,[2] E. Price,[46] J. D. Price,[52] J. Prisciandaro,[39] A. Pritchard,[52] C. Prouve,[46] V. Pugatch,[44] A. Puig Navarro,[39] G. Punzi,[23,t] W. Qian,[4] R. Quagliani,[7,46] B. Rachwal,[26] J. H. Rademacker,[46] B. Rakotomiaramanana,[39] M. Rama,[23] M. S. Rangel,[2] I. Raniuk,[43] N. Rauschmayr,[38] G. Raven,[42] F. Redi,[53] S. Reichert,[54] M. M. Reid,[48] A. C. dos Reis,[1] S. Ricciardi,[49] S. Richards,[46] M. Rihl,[38] K. Rinnert,[52] V. Rives Molina,[36] P. Robbe,[7,38] A. B. Rodrigues,[1] E. Rodrigues,[54] J. A. Rodriguez Lopez,[62] P. Rodriguez Perez,[54] S. Roiser,[38] V. Romanovsky,[35] A. Romero Vidal,[37] J. W. Ronayne,[12] M. Rotondo,[22] J. Rouvinet,[39] T. Ruf,[38] H. Ruiz,[36] P. Ruiz Valls,[66] J. J. Saborido Silva,[37] N. Sagidova,[30] P. Sail,[51] B. Saitta,[15,k] V. Salustino Guimaraes,[2] C. Sanchez Mayordomo,[66] B. Sanmartin Sedes,[37] R. Santacesaria,[25] C. Santamarina Rios,[37] M. Santimaria,[18] E. Santovetti,[24,h] A. Sarti,[18,s] C. Satriano,[25,c] A. Satta,[24] D. M. Saunders,[46] D. Savrina,[31,32] M. Schiller,[38] H. Schindler,[38] M. Schlupp,[9] M. Schmelling,[10] T. Schmelzer,[9] B. Schmidt,[38] O. Schneider,[39] A. Schopper,[38] M. Schubiger,[39]

M.-H. Schune,[7] R. Schwemmer,[38] B. Sciascia,[18] A. Sciubba,[25,s] A. Semennikov,[31] I. Sepp,[53] N. Serra,[40] J. Serrano,[6] L. Sestini,[22] P. Seyfert,[20] M. Shapkin,[35] I. Shapoval,[16,43,b] Y. Shcheglov,[30] T. Shears,[52] L. Shekhtman,[34] V. Shevchenko,[64] A. Shires,[9] R. Silva Coutinho,[48] G. Simi,[22] M. Sirendi,[47] N. Skidmore,[46] I. Skillicorn,[51] T. Skwarnicki,[59] E. Smith,[55,49] E. Smith,[53] I. T. Smith,[50] J. Smith,[47] M. Smith,[54] H. Snoek,[41] M. D. Sokoloff,[57,38] F. J. P. Soler,[51] D. Souza,[46] B. Souza De Paula,[2] B. Spaan,[9] P. Spradlin,[51] S. Sridharan,[38] F. Stagni,[38] M. Stahl,[11] S. Stahl,[38] O. Steinkamp,[40] O. Stenyakin,[35] F. Sterpka,[59] S. Stevenson,[55] S. Stoica,[29] S. Stone,[59] B. Storaci,[40] S. Stracka,[23,j] M. Straticiuc,[29] U. Straumann,[40] L. Sun,[57] W. Sutcliffe,[53] K. Swientek,[27] S. Swientek,[9] V. Syropoulos,[42] M. Szczekowski,[28] P. Szczypka,[39,38] T. Szumlak,[27] S. T'Jampens,[4] T. Tekampe,[9] M. Teklishyn,[7] G. Tellarini,[16,b] F. Teubert,[38] C. Thomas,[55] E. Thomas,[38] J. van Tilburg,[41] V. Tisserand,[4] M. Tobin,[39] J. Todd,[57] S. Tolk,[42] L. Tomassetti,[16,b] D. Tonelli,[38] S. Topp-Joergensen,[55] N. Torr,[55] E. Tournefier,[4] S. Tourneur,[39] K. Trabelsi,[39] M. T. Tran,[39] M. Tresch,[40] A. Trisovic,[38] A. Tsaregorodtsev,[6] P. Tsopelas,[41] N. Tuning,[41,38] A. Ukleja,[28] A. Ustyuzhanin,[65,64] U. Uwer,[11] C. Vacca,[15,k] V. Vagnoni,[14] G. Valenti,[14] A. Vallier,[7] R. Vazquez Gomez,[18] P. Vazquez Regueiro,[37] C. Vázquez Sierra,[37] S. Vecchi,[16] J. J. Velthuis,[46] M. Veltri,[17,u] G. Veneziano,[39] M. Vesterinen,[11] B. Viaud,[7] D. Vieira,[2] M. Vieites Diaz,[37] X. Vilasis-Cardona,[36,f] A. Vollhardt,[40] D. Volyanskyy,[10] D. Voong,[46] A. Vorobyev,[30] V. Vorobyev,[34] C. Voß,[63] J. A. de Vries,[41] R. Waldi,[63] C. Wallace,[48] R. Wallace,[12] J. Walsh,[23] S. Wandernoth,[11] J. Wang,[59] D. R. Ward,[47] N. K. Watson,[45] D. Websdale,[53] A. Weiden,[40] M. Whitehead,[48] D. Wiedner,[11] G. Wilkinson,[55,38] M. Wilkinson,[59] M. Williams,[38] M. P. Williams,[45] M. Williams,[56] T. Williams,[45] F. F. Wilson,[49] J. Wimberley,[58] J. Wishahi,[9] W. Wislicki,[28] M. Witek,[26] G. Wormser,[7] S. A. Wotton,[47] S. Wright,[47] K. Wyllie,[38] Y. Xie,[61] Z. Xu,[39] Z. Yang,[3] J. Yu,[61] X. Yuan,[34] O. Yushchenko,[35] M. Zangoli,[14] M. Zavertyaev,[10,v] L. Zhang,[3] Y. Zhang,[3] A. Zhelezov,[11] A. Zhokhov,[31] and L. Zhong[3]

(LHCb Collaboration)

[1]*Centro Brasileiro de Pesquisas Físicas (CBPF), Rio de Janeiro, Brazil*
[2]*Universidade Federal do Rio de Janeiro (UFRJ), Rio de Janeiro, Brazil*
[3]*Center for High Energy Physics, Tsinghua University, Beijing, China*
[4]*LAPP, Université Savoie Mont-Blanc, CNRS/IN2P3, Annecy-Le-Vieux, France*
[5]*Clermont Université, Université Blaise Pascal, CNRS/IN2P3, LPC, Clermont-Ferrand, France*
[6]*CPPM, Aix-Marseille Université, CNRS/IN2P3, Marseille, France*
[7]*LAL, Université Paris-Sud, CNRS/IN2P3, Orsay, France*
[8]*LPNHE, Université Pierre et Marie Curie, Université Paris Diderot, CNRS/IN2P3, Paris, France*
[9]*Fakultät Physik, Technische Universität Dortmund, Dortmund, Germany*
[10]*Max-Planck-Institut für Kernphysik (MPIK), Heidelberg, Germany*
[11]*Physikalisches Institut, Ruprecht-Karls-Universität Heidelberg, Heidelberg, Germany*
[12]*School of Physics, University College Dublin, Dublin, Ireland*
[13]*Sezione INFN di Bari, Bari, Italy*
[14]*Sezione INFN di Bologna, Bologna, Italy*
[15]*Sezione INFN di Cagliari, Cagliari, Italy*
[16]*Sezione INFN di Ferrara, Ferrara, Italy*
[17]*Sezione INFN di Firenze, Firenze, Italy*
[18]*Laboratori Nazionali dell'INFN di Frascati, Frascati, Italy*
[19]*Sezione INFN di Genova, Genova, Italy*
[20]*Sezione INFN di Milano Bicocca, Milano, Italy*
[21]*Sezione INFN di Milano, Milano, Italy*
[22]*Sezione INFN di Padova, Padova, Italy*
[23]*Sezione INFN di Pisa, Pisa, Italy*
[24]*Sezione INFN di Roma Tor Vergata, Roma, Italy*
[25]*Sezione INFN di Roma La Sapienza, Roma, Italy*
[26]*Henryk Niewodniczanski Institute of Nuclear Physics Polish Academy of Sciences, Kraków, Poland*
[27]*AGH - University of Science and Technology, Faculty of Physics and Applied Computer Science, Kraków, Poland*
[28]*National Center for Nuclear Research (NCBJ), Warsaw, Poland*
[29]*Horia Hulubei National Institute of Physics and Nuclear Engineering, Bucharest-Magurele, Romania*
[30]*Petersburg Nuclear Physics Institute (PNPI), Gatchina, Russia*
[31]*Institute of Theoretical and Experimental Physics (ITEP), Moscow, Russia*
[32]*Institute of Nuclear Physics, Moscow State University (SINP MSU), Moscow, Russia*
[33]*Institute for Nuclear Research of the Russian Academy of Sciences (INR RAN), Moscow, Russia*

[34]Budker Institute of Nuclear Physics (SB RAS) and Novosibirsk State University, Novosibirsk, Russia

[35]Institute for High Energy Physics (IHEP), Protvino, Russia

[36]Universitat de Barcelona, Barcelona, Spain

[37]Universidad de Santiago de Compostela, Santiago de Compostela, Spain

[38]European Organization for Nuclear Research (CERN), Geneva, Switzerland

[39]Ecole Polytechnique Fédérale de Lausanne (EPFL), Lausanne, Switzerland

[40]Physik-Institut, Universität Zürich, Zürich, Switzerland

[41]Nikhef National Institute for Subatomic Physics, Amsterdam, The Netherlands

[42]Nikhef National Institute for Subatomic Physics and VU University Amsterdam, Amsterdam, The Netherlands

[43]NSC Kharkiv Institute of Physics and Technology (NSC KIPT), Kharkiv, Ukraine

[44]Institute for Nuclear Research of the National Academy of Sciences (KINR), Kyiv, Ukraine

[45]University of Birmingham, Birmingham, United Kingdom

[46]H.H. Wills Physics Laboratory, University of Bristol, Bristol, United Kingdom

[47]Cavendish Laboratory, University of Cambridge, Cambridge, United Kingdom

[48]Department of Physics, University of Warwick, Coventry, United Kingdom

[49]STFC Rutherford Appleton Laboratory, Didcot, United Kingdom

[50]School of Physics and Astronomy, University of Edinburgh, Edinburgh, United Kingdom

[51]School of Physics and Astronomy, University of Glasgow, Glasgow, United Kingdom

[52]Oliver Lodge Laboratory, University of Liverpool, Liverpool, United Kingdom

[53]Imperial College London, London, United Kingdom

[54]School of Physics and Astronomy, University of Manchester, Manchester, United Kingdom

[55]Department of Physics, University of Oxford, Oxford, United Kingdom

[56]Massachusetts Institute of Technology, Cambridge, Massachusetts, USA

[57]University of Cincinnati, Cincinnati, Ohio, USA

[58]University of Maryland, College Park, Maryland, USA

[59]Syracuse University, Syracuse, New York, USA

[60]Pontifícia Universidade Católica do Rio de Janeiro (PUC-Rio), Rio de Janeiro, Brazil
(associated with Institution Universidade Federal do Rio de Janeiro (UFRJ), Rio de Janeiro, Brazil)

[61]Institute of Particle Physics, Central China Normal University, Wuhan, Hubei, China
(associated with Institution Center for High Energy Physics, Tsinghua University, Beijing, China)

[62]Departamento de Fisica, Universidad Nacional de Colombia, Bogota, Colombia
(associated with Institution LPNHE, Université Pierre et Marie Curie, Université Paris Diderot, CNRS/IN2P3, Paris, France)

[63]Institut für Physik, Universität Rostock, Rostock, Germany
(associated with Institution Physikalisches Institut, Ruprecht-Karls-Universität Heidelberg, Heidelberg, Germany)

[64]National Research Centre Kurchatov Institute, Moscow, Russia
(associated with Institution Institute of Theoretical and Experimental Physics (ITEP), Moscow, Russia)

[65]Yandex School of Data Analysis, Moscow, Russia
(associated with Institution Institute of Theoretical and Experimental Physics (ITEP), Moscow, Russia)

[66]Instituto de Fisica Corpuscular (IFIC), Universitat de Valencia-CSIC, Valencia, Spain
(associated with Institution Universitat de Barcelona, Barcelona, Spain)

[67]Van Swinderen Institute, University of Groningen, Groningen, The Netherlands
(associated with Institution Nikhef National Institute for Subatomic Physics, Amsterdam, The Netherlands)

[a]Also at Università di Firenze, Firenze, Italy.

[b]Also at Università di Ferrara, Ferrara, Italy.

[c]Also at Università della Basilicata, Potenza, Italy.

[d]Also at Università di Modena e Reggio Emilia, Modena, Italy.

[e]Also at Università di Milano Bicocca, Milano, Italy.

[f]Also at LIFAELS, La Salle, Universitat Ramon Llull, Barcelona, Spain.

[g]Also at Università di Bologna, Bologna, Italy.

[h]Also at Università di Roma Tor Vergata, Roma, Italy.

[i]Also at Università di Genova, Genova, Italy.

[j]Also at Scuola Normale Superiore, Pisa, Italy.

[k]Also at Università di Cagliari, Cagliari, Italy.

[l]Also at Politecnico di Milano, Milano, Italy.

[m]Also at Universidade Federal do Triângulo Mineiro (UFTM), Uberaba-MG, Brazil.

[n]Also at AGH - University of Science and Technology, Faculty of Computer Science, Electronics and Telecommunications, Kraków, Poland.

[o]Also at Università di Padova, Padova, Italy.

[p]Also at Hanoi University of Science, Hanoi, Viet Nam.

[q]Also at Università di Bari, Bari, Italy.

[r]Also at Università degli Studi di Milano, Milano, Italy.

[s]Also at Università di Roma La Sapienza, Roma, Italy.

[t]Also at Università di Pisa, Pisa, Italy.

[u]Also at Università di Urbino, Urbino, Italy.

[v]Also at P.N. Lebedev Physical Institute, Russian Academy of Science (LPI RAS), Moscow, Russia.